Photobiomodulation, Photomedicine, and Laser Surgery
Volume 38, Number 2, 2020

Pp. 115–131
DOI: 10.1089/photob.2019.4630

Increased Functional Connectivity Within Intrinsic Neural Networks in Chronic Stroke Following Treatment with Red/Near-Infrared Transcranial Photobiomodulation: Case Series with Improved Naming in Aphasia

Margaret A. Naeser, PhD,[1,2] Michael D. Ho, PhD,[1] Paula I. Martin, PhD,[1,2]
Michael R. Hamblin, PhD,[3–5] and Bang-Bon Koo, PhD[6]

Abstract

Objective: To examine effects of four different transcranial, red/near-infrared (NIR), light-emitting diode (tLED) protocols on naming ability in persons with aphasia (PWA) due to left hemisphere (LH) stroke. This is the first study to report beneficial effects from tLED therapy in *chronic* stroke, and parallel changes on functional magnetic resonance imaging (fMRI).

Materials and methods: Six PWA, 2–18 years poststroke, in whom 18 tLED treatments were applied (3×/week, 6 weeks) using LED cluster heads: 500 mW, red (633 nm) and NIR (870 nm), 22.48 cm^2, 22.2 mW/cm^2.

Results: After Protocol A with bilateral LED placements, including midline, at scalp vertex over left and right supplementary motor areas (L and R SMAs), picture naming was not improved. P1 underwent pre-/postovert, picture-naming *task-fMRI* scans; P2 could not. After Protocol A, P1 showed increased activation in LH and right hemisphere, including L and R SMAs. After Protocol B with LEDs *only* on ipsilesional, LH side, naming ability significantly improved for P1 and P2; the fMRI scans for P1 then showed activation *only* on the ipsilesional LH side. After Protocol C with LED placements on ipsilesional LH side, plus *one midline placement* over mesial prefrontal cortex (mPFC) at front hairline, a cortical node of the default mode network (DMN), P3 and P4 had only moderate/poor response, and no increase in functional connectivity on resting-state functional-connectivity MRI. After Protocol D, however, with LED placements on ipsilesional LH side, plus over *two midline nodes of DMN*, mPFC, and precuneus (high parietal) *simultaneously*, P5 and P6 each had good response with significant increase in functional connectivity within DMN, $p < 0.0005$; salience network, $p < 0.0005$; and central executive network, $p < 0.05$.

Conclusions: NIR photons can affect surface brain cortex areas subjacent to where LEDs are applied on the scalp. Improved naming ability was present with optimal Protocol D. Transcranial photobiomodulation may be an additional noninvasive therapy for stroke.

Keywords: stroke, aphasia treatment, PBM, default mode network, functional connectivity, fMRI

[1]VA Boston Healthcare System (12-A), Boston, Massachusetts.
[2]Department of Neurology, Boston University School of Medicine, Boston, Massachusetts.
[3]Wellman Center for Photomedicine, Massachusetts General Hospital, Boston, Massachusetts.
[4]Department of Dermatology, Harvard Medical School, Boston, Massachusetts.
[5]Harvard-MIT Division of Health Sciences and Technology, Cambridge, Massachusetts.
[6]Brain-Imaging and Informatics Lab (BIL), Department of Anatomy and Neurobiology, Boston University School of Medicine, Boston, Massachusetts.

Parts of this article were presented at Academy of Aphasia Meeting, San Francisco, October 2012, and International Neuropsychological Society Meeting, Boston, February 2016:

Naeser MA, Ho MD, Martin PI, Treglia E, Krengel MH, Hamblin MR, Baker EH. Improved language after scalp application of red/near-infrared light-emitting diodes: Pilot study supporting a new, noninvasive treatment for chronic aphasia. Poster presented at the Academy of Aphasia, October 28, 2012, San Francisco, California.

Ho MD, Martin PI, Yee MK, Koo BB, Baker E, Hamblin MR, Naeser MA. Increased functional connectivity in default mode network associated with application of transcranial, light-emitting diodes to treat chronic aphasia: case series. Poster presented at the International Neuropsychological Society Meeting, February 6, 2016, Boston, Massachusetts.

Introduction

PHOTOBIOMODULATION (PBM) THERAPY IS a safe, painless, noninvasive, nonthermal modality using primarily visible red and/or near-infrared (NIR) wavelengths, ~600–1100 nm to stimulate, heal, and repair damaged or dying cells and tissues.[1–3] Multiple effects are associated with application of red/NIR PBM to hypoxic/compromised cells. These include increased local vasodilation after release of nitric oxide from cytochrome C oxidase in mitochondria of hypoxic cells, and increased production of adenosine triphosphate (ATP). After application of NIR light-emitting diodes (LED) to the forehead, increased local regional cerebral blood flow (rCBF) in the frontal pole cortex areas, and improved behavior have been reported in major depressive disorder[4] and severe traumatic brain injury (TBI).[5] Increased overall rCBF was present on brain single-photon emission computerized tomography scans in veterans with chronic TBI,[6] and focal increases were observed in pilot reports with chronic stroke patients.[7,8]

After exposure to red/NIR photons, there is a brief burst of reactive oxygen species that induces redox-sensitive transcription factors including nuclear factor-kappa B (NF-κB) that promote gene transcription, including activation of secondary antioxidant mechanisms that result in a net reduction of oxidative stress.[9,10] Two genes that are upregulated after NF-κB activation include those for mitochondrial superoxide dismutase, a powerful antioxidant[11] and heat-shock protein 70, a molecular chaperone for protein molecules that prevents misfolding and unwanted protein aggregation that is neuroprotective.[12]

In small-animal studies, transcranial PBM (tPBM) was observed to have an anti-inflammatory effect in the brain in acute TBI, as well as in Alzheimer's disease (AD) mice.[13–16] In acute TBI, increased brain-derived neurotrophic factor (BDNF) was present at day 7 (promoting neurogenesis) when NIR tPBM was started at 4 h post-TBI, for 3 days. At day 28, there was increased Synapsin-1 (promoting synaptogenesis), along with improved behavior.[17,18]

TPBM has improved cognition in chronic TBI in humans.[19] The red/NIR LEDs were placed on the head (midline, from front-to-back hairline; bilaterally on frontal, parietal, and temporal areas). These scalp placements included, in part, cortical nodes of the intrinsic neural network, the default mode network (DMN)—for example, mesial prefrontal cortex (mPFC) and precuneus, as well as the L and R inferior parietal cortex (intraparietal sulcus/angular gyrus areas).[19,20] The DMN is active during daydreaming, but must downregulate, in order for goal-directed tasks (executive function) to take place. The DMN is dysregulated in TBI, likely due to the twisting and shearing of white matter axons associated with TBI.[21] Significant improvements in executive function and verbal memory were observed after 18 transcranial LED (tLED) treatments (3×/week, 6 weeks), with improvements lasting out to 2 months after the final treatment. In addition to improved cognition, the TBI participants reported improved sleep. The red wavelength has been shown to increase melatonin.[22] Fewer post-traumatic stress disorder (PTSD) symptoms were also reported.[19,20] Chronic PTSD shares some of the same abnormal neurocircuitry with chronic TBI, including mPFC dysfunction. The mPFC is important for top-down governance of the amygdala to modulate emotional outbursts.[23]

TPBM has improved cognition in mild to moderately severe dementia cases.[24,25] The DMN is dysregulated in AD.[26–29] The cortical nodes of the DMN (especially mPFC) have high demand for glucose and energy.[30,31] In both dementia studies,[24,25] the tPBM treatments included LED placements over *only* cortical nodes of the DMN. In addition, a NIR LED noseclip was placed in a nostril, hypothesized to deliver NIR photons to the olfactory bulbs (on orbitofrontal cortex) with direct connections to parahippocampal areas.[32] There were significant improvements after 12 weeks of tPBM—for example, MMSE, $p < 0.003$; and the Alzheimer's Disease Assessment Scale-Cognition (ADAS-Cog), $p < 0.023$.[24] Better sleep, fewer angry outbursts, and fewer episodes of wandering were reported by families. Precipitous declines were observed, however, during the follow-up 4-week no-treatment period (weeks 12 to 16) in these cases with a progressive neurodegenerative disease.[24] These results with dementia were in juxtaposition to the continued cognitive improvements observed at 2 months after the final tPBM treatment with chronic TBI cases.[19,20]

TPBM was used to treat *acute* human stroke in the NeuroThera Effectiveness and Safety Trial (NEST).[33–35] Patients received only one tPBM treatment, at <24 h post-stroke onset, and placements followed the 10/20 electroencephalography (EEG) system over the left hemisphere (LH) plus over the right hemisphere (RH), regardless of the side of stroke. There was significant improvement on the NIH Stroke Severity Scale (NIHSSS) in the real, but not in the sham-treated groups. When the NEST tPBM protocol was extended into Phase III clinical trials, however, it failed to reach significance at the interim analysis point and the study was suspended. Some possible contributing factors for this are presented in the Discussion section.

Neurogenesis persists in the adult mammalian brain[36] and is upregulated after ischemia and brain injury.[37] Mitochondrial dysfunction inhibits adult neurogenesis.[38] Thus, improving mitochondrial function with NIR tPBM would be desirable, not only to promote increased ATP and rCBF, but also to possibly promote some adult neurogenesis.

Since 1981, the depth of brain penetration from scalp surface with NIR laser in human cadavers has been studied.[39] Photons from an 808 nm laser have been detected at a depth of 4–5 cm.[40] The effect is nonthermal.[41] There have been no negative side effects reported in animal or human studies since research and clinical studies began in the 1960s.[42] PBM offers the possibility of endogenous self-repair mechanisms.

The purpose of this case series report was to examine the effects of red/NIR tPBM on language and functional magnetic resonance imaging (fMRI) scans in persons with aphasia (PWA) due to LH stroke. Four different tLED protocols were examined. Part 1 (Protocols A and B) examined which side/s of the head/brain to optimally treat (*bilateral* LED placements vs. *ipsilesional, only LH* placements). Part 2 (Protocols C and D) examined the effect of LED placements over only the LH, plus *one midline node of the DMN* (mPFC) versus *two midline nodes of the DMN* (mPFC plus precuneus), and the effect of dosage applied to each placement area (13 vs. 26 J/cm^2).

Methods

Participants

Demographics for each right-handed PWA are provided in Table 1. Six males, ages 46–49 years, participated at 2–18

Table 1. Demographics for Six (Males) Left Hemisphere Stroke Patients with Chronic Aphasia Treated with Transcranial Light-Emitting Diode Protocols A, B, C, or D

Patient ID no.	*Age at entry into study, years*	*Time poststroke at entry into study, years*	*Years educ.*	*Stroke history*	*Right-sided paralysis?*	*Aphasia type*	*Handedness*	*Other*	*Treated with specific transcranial, LED treatment protocol: A, B, C, or D*
Part 1									
P1	67	18	17	L MCA ischemic stroke	R Hemiplegia	Mild–moderate nonfluent, Broca's	Right	Had received rTMS to suppress the R pars triangularis at 10 years. poststroke; GR at that time, lasting 3.7 years	A. Bilateral LH and RH LED placements (both SMAs). 13 J/cm^2 *first LED series* B. LH only *(ipsilesional)* LED placements (no SMAs). 39 J/cm^2 *second LED series*
P2	59	14	16	Tear in carotid artery resulting in L hemorrhage	R Hemiplegia	Moderate nonfluent Broca's	Right		A. Same as above *first LED series* B. Same as above *second LED series*
Part 2									
P3	58	10	16	L MCA ischemic stroke	R Hemiplegia	Recovered nonfluent Broca's with anomia	Right		C. LH LED placements, plus 1 midline node on DMN (mPFC). 13 J/cm^2
P4	46	2	16	L hemorrhage	R Hemiplegia	Recovered nonfluent Broca's with anomia	Right	History of severe depression, and completed the 18 LED treatments for a 12-week period, instead of the usual 6 weeks.	C. Same as above
P5	63	11	20	Mitral valve replacement, with embolic LH stroke	R hand weakness, fourth digit only	Word deafness, rare form, unilateral LH stroke	Right		D. LH LED placements, plus two midline nodes on DMN (mPFC and precuneus). 26 J/cm^2
P6	69	13	20	L MCA ischemic stroke	R Hemiplegia	Mild–moderate nonfluent Broca's	Right		D. Same as above

DMN, default mode network; educ., education; GR, good response; J/cm^2, Joules per cm^2 (fluence or energy density dose delivered); LED, light-emitting diode; LH, left hemisphere; MCA, middle cerebral artery; mPFC, mesial prefrontal cortex; RH, right hemisphere; rTMS, repetitive transcranial magnetic stimulation; SMA, supplementary motor area.

years after single LH stroke. Figure 1 shows the LH areas of infarction for each PWA on T1-weighted structural MRI scans.

Language testing

Each PWA was administered the Boston Diagnostic Aphasia Exam (BDAE)[43] within 1 month before participation to establish the type of aphasia. The primary outcome variable was naming ability. Within 2 weeks before the first tLED treatment, the Boston Naming Test (BNT)[44] and the Philadelphia Naming Test (PNT)[45] were administered three times to each PWA, to establish a baseline mean and standard deviation (SD) for each naming test, for that PWA. If the PWA scored near ceiling for picture naming (BNT and/or PNT) at baseline, then the timed, Benton Controlled Oral Word Association Test (Letters, FAS test),[46] and the verbal fluency/category-naming test for animals (BDAE)[43] were used instead. Each category was timed for 1 min, where the PWA was asked to name aloud as many words as possible, within that category. Post-testing was obtained at 1 or 2 weeks after the 18th tLED treatment, and again at 1 and 2 months later. A change from baseline of 2SD at a post-testing time point was considered significant ($p = 0.05$).

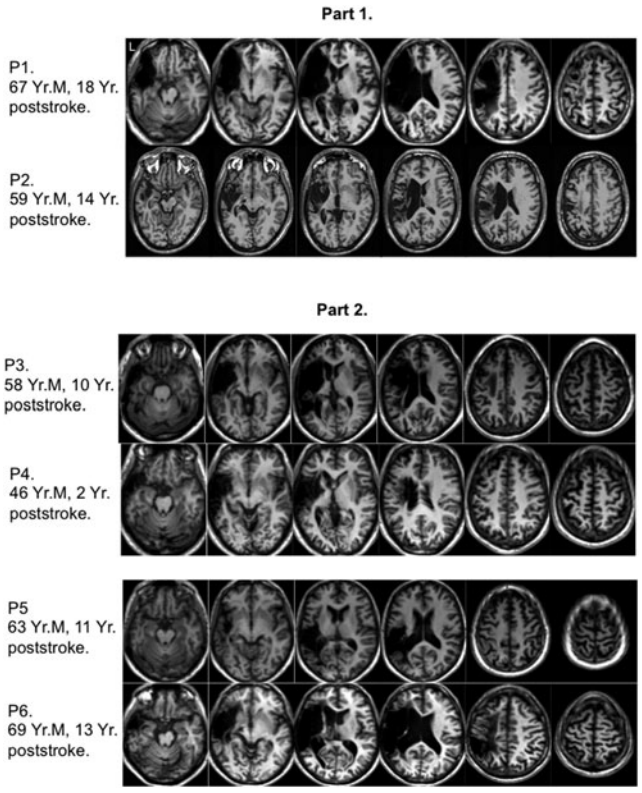

FIG. 1. Axial T1-weighted structural MRI scans for each person with aphasia, P1–P6. The nonfluent aphasia cases (P1, P2, P3, P4, and P6) each had white matter lesions near ventricle, which were compatible with nonfluent aphasia[81]—that is, lesion located anterolateral to the left frontal horn, deep to Broca's area, including medial subcallosal fasciculus with pathways from L SMA and anterior cingulate to head of caudate, and in the middle periventricular white matter area, lateral to body of lateral ventricle (deep to sensorimotor cortex areas for mouth). The white matter lesion anterolateral to left frontal horn likely also included fibers of the aslant tract.[59,82] The fluent aphasia case (P5, with rare, unilateral word deafness)[78] had left temporoparietal lesion, including Wernicke's area, plus lesion adjacent to posterior rim of body of left lateral ventricle, interrupting auditory callosal fibers from right temporal lobe.[79] See also Supplementary Fig. S1. MRI, magnetic resonance imaging; SMA, supplementary motor area.

LED equipment and treatment schedule

The nonsignificant risk FDA-cleared MedX Health (Toronto) Model 1100 LED cluster heads were used in all four LED Protocols (A, B, C, and D). Although many different wavelengths have been shown to be active in PBM, the two wavelengths used in this study, 633 nm and 870 nm in each LED cluster head, are close to two of the four wavelength groups identified by Tiina Karu in a study of the action spectrum of HeLa cell adhesion *in vitro*.[47]

Specific LED parameters are provided in Table 2. Each protocol applied 18 tLED treatments, 3×/week with at least 48 h between treatments (Monday, Wednesday, and Friday) for 6 weeks, during outpatient visits to the VA Boston Healthcare System (VABHS). See Fig. 2.

The LED treatment portion was approved by the Institutional Review Board of the VABHS, where the LED treatments took place. The MRI scan portion was approved by the Institutional Review Boards of both the Boston University School of Medicine, where the MRI scans took place, and the VABHS. Each participant signed informed consent forms from both institutions, and all methods were performed in accordance with the relevant guidelines and regulations. This was an open-protocol exploratory study.

Part 1: Method

Protocol A: Bilateral (LH and RH) LED placements, and midline placements including both L and R supplementary motor areas (SMAs) at vertex. Protocol A LED placements (Table 3) are similar to those used in our TBI studies.[19,20] Two MedX Health (Toronto) Console Model 1100 LED units were used, permitting up to six tLED placements *simultaneously*. Two sequential placement sets of five or six LED cluster heads were applied at each treatment visit. The LED cluster heads were secured in place with a soft nylon cap (Fig. 2).

P1 performed overt picture-naming *task-fMRI* scans pre/post the Protocol A treatment series. The MRI acquisition parameters for structural and fMRI scans are provided in Supplementary Data S1. P2 was unable to undergo 3 Tesla fMRI, due to the type of stents that had been placed postmyocardial infarction.

Protocol B: Only LH ipsilesional LED placements. Within a few weeks after completing post-testing for Protocol A, P1 and P2 were each treated with Protocol B (Tables 2 and 3), where LEDs were placed *only* on the LH *ipsilesional side*. There were no RH placements, no midline placements, including no placement over both L and R SMAs at the midline vertex. P1 again underwent post-LED overt picture-naming *task-fMRIs*.

Table 2. Parameters for Light-Emitting Diode Cluster Heads (MedX Health, Toronto) Used for Each Light-Emitting Diode Protocol: A, B, C, and D

	Parameters for each LED cluster head (MedX Health, Toronto)	*Protocol A*	*Protocol B*	*Protocol C*	*Protocol D*
LED cluster head size	22.48 cm^2 5.34 cm diameter				
Power output	500 mW				
Power density	22.2 mW/cm^2				
No. of red LEDs, 633 nm	9				
No. of NIR LEDs, 870 nm	52				
Mode: PW or CW		PW, 146 Hz	PW, 146 Hz	CW	CW
No. of sec required to reach 1 J/cm^2	45 sec, CW	56.2 sec, PW	56.2 sec, PW	45 sec, CW	45 sec, CW
No. of LED cluster head placements, per session		12	6	9	8
Total fluence per LED placement		13 J/cm^2	39 J/cm^2	13 J/cm^2	26 J/cm^2
Time per LED placement, per session		12 min, 11 sec	36 min, 33 sec	9 min, 45 sec	19 min, 30 sec
Total time duration of LED session		24 min, 22 sec	36 min, 33 sec	19 min, 30 sec	39 min, 0 sec
Total fluence delivered, across the 18 LED treatment sessions		2808 J/cm^2	4212 J/cm^2	2106 J/cm^2	3744 J/cm^2

LED placement locations were different for each of the four protocols (Table 3).
CW, continuous wave; NIR, near-infrared; PW, pulsed wave.

Part 2: Method

The results from Part 1 indicated that improved naming was limited to LED placements on *only* the LH, *ipsilesional side,* and *not both sides*. Thus, in Part 2 *only the LH side* was treated, with four other PWA (P3–P6). The effects of adding one versus two midline LED placements over cortical nodes of the DMN (mPFC, precuneus) and fluence delivered (13, 26 J/cm^2) were examined. Each PWA (P3–P6) participated in resting-state functional-connectivity MRI (rs-fcMRI) scans pre/post one LED treatment series.

Rationale for rs-fcMRI scans

The *rs-fcMRI scans* have become more widely used than *task-fMRI* scans to study stroke recovery because they require no speech or motor movements during fMRI scan acquisition. During rs-fcMRI, the participant is lying in the scanner, resting, and merely looking at a white dot on a black background for 7 min. He/she is instructed to think of nothing in particular, but to keep the eyes open. The rs-fcMRI scans provide information on the strength of functional connections, or correlations, between pairs of specific cortical regions of interest (ROIs), within a specific neural network. For normal brain function to occur, the cortical nodes within a neural network need to have a high degree of correlated temporal oscillations among themselves, during activation (or deactivation). The cortical nodes have very slow, yet coherent, temporal oscillations (only 0.01 to 0.08 Hz), repeating one cycle every 12.5 to 100 sec during rest. There is a range of possible correlation coefficients from −1.0 to +1.0 (Pearson's *r*). Higher positive correlations suggest that the cortical nodes within a specific network are functionally connected—that is, have temporally coherent oscillations. The DMN is often dysregulated (without

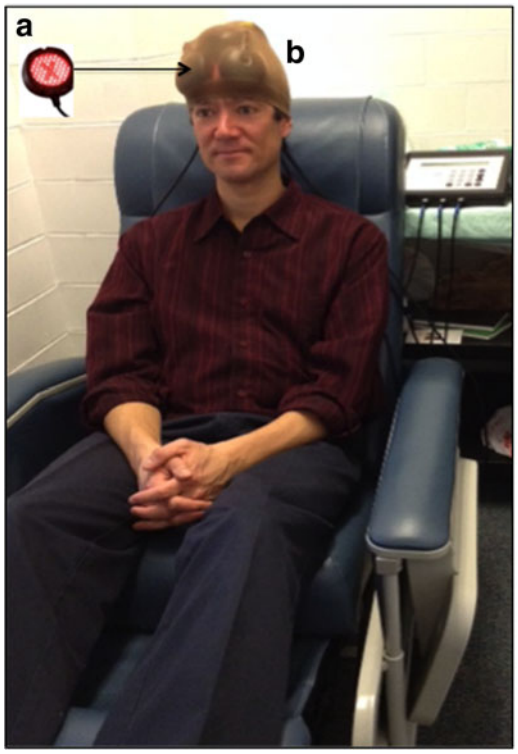

FIG. 2. **(a)** Sample LED cluster head applied to the skin/scalp. The ''X'' indicates location of the nine red LEDs embedded within the LED cluster head. The 52 near-infrared LEDs surrounding the ''X'' are not visible to the eye. **(b)** Subject treated in recliner chair, showing some LED placements used in Protocol A—Bilateral (LH and RH) LED placements, including the L and R SMAs at midline vertex of the head. The LED cluster heads were held in place with a soft nylon cap. LED, light-emitting diode; LH, left hemisphere. Reprinted with author's permission, Naeser et al.[19]

Table 3. Placement Locations on the Scalp for Each Light-Emitting Diode Cluster Head, for Protocols (A, B, C, and D), Including Fluence Delivered, and Mode (Pulsed Wave in Hz, or Continuous Wave)

		Part 1						*Part 2*					
		J/cm^2 (and mode, pulsed Hz; or CW) delivered at each LED cluster head placement											
		Protocol A			*Protocol B*			*Protocol C*			*Protocol D*		
		Bilateral and both SMAs			*LH only no SMAs*			*LH plus 1 node DMN*			*LH plus 2 nodes DMN*		
		13 J/cm^2, 146 Hz			*39 J/cm^2, 146 Hz*			*13 J/cm^2, CW*			*26 J/cm^2, CW*		
		$\sum = 2808\ J/cm^2$			*$\sum = 4212\ J/cm^2$*			*$\sum = 2106\ J/cm^2$*			*$\sum = 3744\ J/cm^2$*		
		Midline			*Midline*			*Midline*			*Midline*		
LED cluster head placement	*Surface brain cortex area targeted to receive photons*	*L*	*L&R*	*R*	*L*	*L&R*	*R*	*L*	*L&R*	*R*	*L*	*L&R*	*R*
On midline of face, centered over front hairline (half of LED cluster head placed anterior to hairline on forehead; half of LED cluster head, posterior to hairline).	mPFC, part of DMN		X						X			X	
On forehead, centered above pupil line between eyebrow and front hairline.	Orbitofrontal cortex, and most anterior middle frontal gyrus areas	X		X	X			X			X		
On midline, *superior* to external occipital protuberance (half-way to vertex of head), and on alternate treatment days, midline, *inferior* to external occipital protuberance.	Precuneus, with midline placement *superior* to occipital protuberance. Precuneus, part of DMN Cerebellum (midline), with midline placement *inferior* to occipital protuberance		X*						Cerebellum only			Precuneus treated each time, and cerebellum, each time	
On midline vertex of the head.	SMAs and possibly pre-SMAs. Pre-SMAs, part of SN		X										
On sole of foot (proximal to toes), alternating L&R on different treatment days, as well as alternating with a placement on dorsum of foot (proximal to toes), also alternating L&R side on different treatment days.	Research with low-level laser light applied to the foot, reported to increase ipsilateral regional cerebral blood flow[83]	(X)*		(X)*									

(*continued*)

TABLE 3. (CONTINUED)

		Part 1						*Part 2*					
		J/cm² (and mode, pulsed Hz; or CW) delivered at each LED cluster head placement											
		Protocol A			*Protocol B*			*Protocol C*			*Protocol D*		
		Bilateral and both SMAs			*LH only no SMAs*			*LH plus 1 node DMN*			*LH plus 2 nodes DMN*		
		13 J/cm², 146 Hz			*39 J/cm², 146 Hz*			*13 J/cm², CW*			*26 J/cm², CW*		
		∑ = 2808 J/cm²			*∑ = 4212 J/cm²*			*∑ = 2106 J/cm²*			*∑ = 3744 J/cm²*		
		Midline			*Midline*			*Midline*			*Midline*		
LED cluster head placement	*Surface brain cortex area targeted to receive photons*	*L*	*L&R*	*R*	*L*	*L&R*	*R*	*L*	*L&R*	*R*	*L*	*L&R*	*R*
Immediately *posterior* to front hairline, centered on pupil line	Middle frontal gyrus areas, including dorsolateral prefrontal cortex, part of CEN	X		X	X			X					
Temple area	Inferior frontal gyrus (Broca's) area, possibly including anterior insula (AI), unknown due to greater depth of AI. AI, part of SN	X		X	X			X			X		
Posterior, superior to each ear	Posterolateral inferior parietal cortex (angular gyrus area), part of DMN	X		X	X			X			X		
Immediately *superior* to tip of ear	Posterior superior temporal gyrus (Wernicke's) area				X			X			X		
Immediately superior to the Wernicke's area placement	Lower sensorimotor cortex (mouth) areas				X			X					
On mastoid process (behind ear)	Posterior middle temporal gyrus area and fusiform gyrus area							X			X		

A single LED cluster head applied to a *midline placement* covered both the left and right target cortical areas for that placement, due to the 5.34 cm diameter of the LED cluster head (22.48 cm^2). See Table 2, for more LED parameters.

*Used on alternating treatment days.

(X) indicates left side OR right side

AI, anterior insula; CEN, central executive network; PW, pulsed wave in Hz; SN, salience network; t-LED, transcranial light-emitting diode.

temporally coherent oscillations, and with low correlation coefficients) in disorders such as TBI and AD.[21,25,26,28,29]

The DMN is of particular interest because it controls other networks. For example, the DMN needs to deactivate (downregulate itself) when other neural networks need to activate (upregulate) to allow normal brain function for various tasks. This is particularly important for executive function (decision-making, planning, and multi-tasking), requiring activation of the dorsolateral prefrontal cortex and intraparietal sulcus, cortical areas, parts of the central executive network (CEN). In this study, rs-fcMRI scans were used to examine functional connectivity in three intrinsic neural networks—for example, the DMN; the salience network (SN) that drives the DMN; and the CEN, important for executive function. The language network could not be studied, due to heterogeneity of the LH lesion sites. More information on rs-fcMRI scan acquisition parameters and analysis programs is given in Supplementary Data S1.

Protocol C. Only LH, plus one midline cortical node of DMN (mPFC) using 13 J/cm^2. P3 and P4 were treated with LED Protocol C (Tables 2 and 3).

Protocol D: Only LH, plus two midline cortical nodes of DMN (mPFC and precuneus) using 26 J/cm^2. P5 and P6 were treated with Protocol D (Tables 2 and 3).

Results

Part 1: Results

Protocol A: Bilateral (LH and RH) LED placements, and midline placements including both L and R SMAs at vertex. After Protocol A, picture naming was significantly impaired on the PNT for P1; scores were also lower for P2 (Table 4, top). (BNT scores were not available for these first two cases.) The *percent change from Baseline* for PNT-naming scores post-Protocol A is shown in red on bar graphs (Fig. 3).

After Protocol A, the overt picture-naming *task-fMRI* scans for P1 showed increased activation in the LH perilesional areas, and in the RH, post- the 18th bilateral LED treatment compared with pre-LED treatment (Fig. 3, top row, left side). This included high activation in R frontal, temporal, and parietal contralesional areas, *plus* in both the R and L SMAs at midline, vertex. All of these cortical areas had been treated with the LEDs.

Protocol B: Only LH ipsilesional LED placements. After Protocol B, picture-naming scores for P1 and P2 were significantly improved on the PNT (Table 4, bottom). The *percent change from Baseline* for the PNT naming scores post-Protocol B is shown in green on bar graphs (Fig. 3).

After Protocol B, the overt picture-naming *task-fMRI* scans for P1 showed increased activation primarily on the *ipsilesional LH side* (the side treated with LEDs), and in the L SMA, despite no direct treatment to the L SMA (Fig. 3, top row, right side). There are connections between the L SMA, and LH language and motor cortex areas, addressed in the Discussion section. There was little or no activation in R frontal, temporal, parietal, and contralesional areas, nor the R SMA; these RH areas were not treated with the LED cluster heads in Protocol B.

Part 2: Results

Part 2: Definitions of response levels for naming, post-LED. In Part 2, it was possible to define different response levels after each tLED treatment series—for example, good, moderate, or poor. Good response (GR) was defined as an increase of +2SD from baseline, on at least two of the six post-LED test scores. Moderate response (MR) was defined

Table 4. Part 1: Pre/Post, Naming Test Scores for Protocol A (Top), and for Protocol B (Bottom), for P1 and P2

Part 1: Naming test scores				
Protocol A: Bilateral (LH and RH) LED placements, and both L and R SMAs				
	Baseline mean (SD)	*1 week Post-18th Tx.*	*1 month Post-18th Tx.*	*2 months Post-18th Tx.*
P1 *(first LED series)* Picture naming PNT (Max = 50)	25.33 (1.53)	25	22 (−)*	26
P2 *(first LED series)* Picture naming PNT (Max = 50)	5.00 (2.00)	6	3	5
Protocol B: Ipsilesional, only LH LED placements				
P1 *(second LED series)* Picture naming PNT (Max = 50)	25.33 (1.53)	27	29 (+)*	25
P2 *(second LED series)* Picture naming PNT (Max = 50)	5.00 (2.00)	9 (+)*	8	7

*$p < 0.05$ (±2 SD post-LED, relative to three baseline testing sessions, pre-LED).
PNT, Philadelphia Naming Test; SD, standard deviation; Tx., treatment.

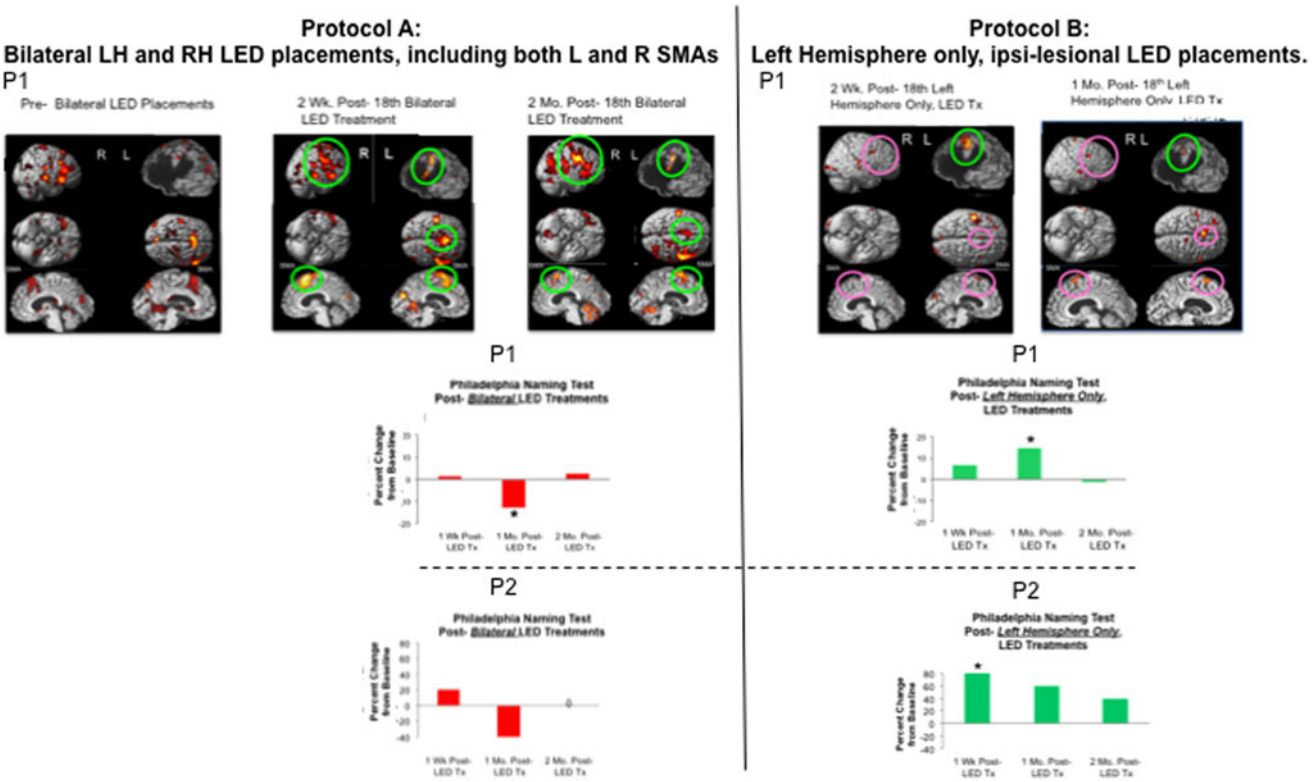

FIG. 3. Part 1: After Protocol A (top row, left side), the overt picture-naming *task-fMRI* scans for P1 showed increased activation (green circles) in the LH perilesional area, and in the RH, post- the 18th bilateral LED treatment, compared with pre-LED. This included high activation in R frontal, temporal, and parietal, contra-lesional cortical areas, *plus* in both the R and L SMAs at midline vertex of the brain. All of these cortical areas had been treated with the LEDs. After Protocol A, the red bar graphs (left side), showing percentage change in naming from baseline, indicated decreased naming for P1 and P2. After Protocol B (top row, right side), the overt picture-naming *task-fMRI* scans for P1, especially at 2 weeks post-LED, showed primarily increased activation only in the LH perilesional area (green circle). Other areas with change after Protocol B compared with Protocol A are marked with pink circles. After Protocol B, the green bar graphs (right side) indicated increased naming for P1 and P2. The activation patterns on the overt picture-naming *task-fMRI* scans for P1, after Protocol B compared with Protocol A, suggested that the two different LED placement sets affected different surface brain cortex areas, subjacent to the different LED scalp placement locations. As a result, there were different effects on naming post-LED—that is, Protocol A with *bilateral placements* was associated with no improvement in naming; however, Protocol B with *only LH ipsilesional placements* was associated with significant improvement in naming. $*p < 0.05$.

as significant increase on some of the post-LED test scores, but also a decrease of −2SD on any of the post-LED test scores. Poor response (PR) was defined as no significant increase on any of the six post-LED test scores.

The six post-LED test scores were comprised of the following: there were three post-LED testing time points—for example, at 1 or 2 weeks after the 18th LED treatment, and at 1 month and 2 months later. For each of these three post-LED testing time points, each PWA had naming data for two naming tests—for example, for either two *picture-naming* tests (BNT, PNT), or for two *verbal fluency/category-naming* tests (Letters FAS test; Animals). Thus, for each PWA, there was a total of six post-LED test scores.

Protocol C: Only LH plus one midline cortical node of DMN (mPFC) using 13 J/cm^2. After Protocol C, P3 and P4 each had only MR or PR, respectively (Table 5, top). P4 had a history of severe depression; he required 12 weeks to complete the 18 tLED treatments compared with 6–7 weeks for the other participants.

After Protocol C, these MR/PR cases showed no significant increase in functional connectivity on the rs-fcMRI scans in the neural networks examined—for example, DMN, SN, and CEN. The rs-fcMRI scan correlation matrices pre-/post-LED for P3 and for P4 are shown in Fig. 4. Statistical analyses for these pre/post comparisons in functional connectivity are provided in Table 6.

Protocol D: Only LH plus two midline cortical nodes of DMN (mPFC and precuneus) using 26 J/cm^2. After Protocol D, P5 and P6 each had significant improvements (GR) on post-LED naming test scores (Table 5, bottom).

After Protocol D, P5 and P6 also showed significant increase in functional connectivity on rs-fcMRI scans in the three neural networks examined—for example, DMN ($p < 0.0005$), SN ($p < 0.0005$), and CEN ($p < 0.05$). See rs-fcMRI correlation matrices pre-/post-LED for P5 and for P6 (Fig. 5). Statistical analyses for these pre/post comparisons in functional connectivity are provided in Table 6.

TABLE 5. PART 2: PRE/POST NAMING TEST SCORES FOR PROTOCOL C (TOP), P3, AND P4; AND FOR PROTOCOL D (BOTTOM), P5, AND P6

Part 2: Naming test scores				
Protocol C: LH, plus one midline cortical node of DMN (mPFC)				
	Baseline mean (SD)	*1 week post-18th Tx.*	*1 month post-18th Tx.*	*2 month Post-18th Tx.*
P3 (moderate response)				
Category naming				
Words begin with letters F, A, or S	11.00 (3.46)	17	12	13
Total F, A, S				
Animals	9.00 (0.00)	10 (+)	10 (+)	5 (–)
P4 (poor response)				
Category naming				
Words begin with letters F, A, or S	13.67 (6.66)	23	13	19
Total F, A, S				
Animals	14.33 (1.53)	16	16	12
Protocol D: LH, plus two midline cortical nodes of DMN (mPFC and precuneus)				
P5 (good response)				
Category naming				
Words begin with letters F, A, or S	46.33 (3.79)	45	58 (+)*	44
Total F, A, S				
Animals	20.00 (1.00)	22 (+)*	21	20
P6 (good response)				
Picture naming				
BNT (max = 60)	33.67 (0.58)	40 (+)*	43 (+)*	42 (+)*
PNT (max = 50)	26.00 (2.75)	22	36 (+)*	29

If person with aphasia was already near ceiling on picture naming (PNT and BNT) at baseline, then verbal fluency/category naming (letters, FAS test; and animals) was used as the primary outcome measure.

*$p < 0.05$ (±2 SD post-LED, relative to three baseline testing sessions, pre-LED).

BNT, Boston Naming Test.

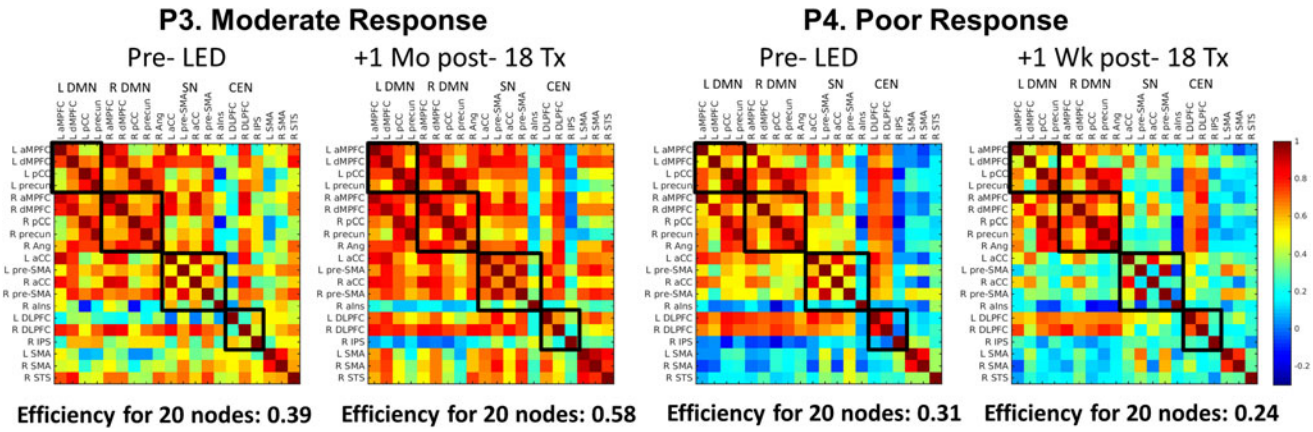

FIG. 4. Part 2: Pre/post rs-fcMRI scan correlation matrices for 20 cortical ROIs for Protocol C, for case P3, MR, and case P4, PR (Table 5, top, naming test scores). These two cases did not show significant increase in functional connectivity within the DMN, SN, or CEN, post-18 tLED treatments (Table 6). With Protocol C, the LED cluster heads were placed only on the LH, the ipsilesional side, *plus one midline node on the DMN*—for example, mPFC, with 13 J/cm^2 per LED placement. The *pre-LED* node efficiency, which assessed the connectedness of the edges for the 20 ROI nodes, ranged from 0.39 (P3) to only 0.31 (P4). The *post-LED* efficiency increased for P3 to 0.58 (change of +0.19), but for P4, it decreased to 0.24 (change of –0.07). P4 required 12 weeks to complete the 18 tLED treatments, often receiving only one treatment per week. CEN, central executive network; DMN, default mode network; mPFC, mesial prefrontal cortex; MR, moderate response; PR, poor response; ROIs, regions of interest; rs-fcMRI, resting-state functional-connectivity MRI; SN, salience network; tLED, transcranial LED.

Table 6. Part 2: Paired *t*-Test Results for Pearson's *r* Correlations Transformed into z-Scores for Cortical Regions of Interest in the Default Mode, Salience and Central Executive Networks, Pre/Post Protocols C and D

	Protocol C		*Protocol D*	
	Mod./poor responders		*Good responders*	
	Pre-	*Post-*	*Pre-*	*Post-*
DMN				
Mean	0.93	0.97	0.84	1.17
SD	0.39	0.38	0.40	0.31
SE	0.05	0.05	0.05	0.04
df	71		71	
t-stat	−1.87		−11.35	
p	0.0653		0.0000	
SN				
Mean	0.66	0.64	0.75	1.07
SD	0.45	0.51	0.40	0.39
SE	0.10	0.12	0.09	0.09
df	19		19	
t-stat	0.39		−5.94	
p	0.7021		0.0000	
CEN				
Mean	0.44	0.47	0.57	1.18
SD	0.42	0.30	0.45	0.47
SE	0.17	0.12	0.18	0.19
df	5		5	
t-stat	−0.23		−3.54	
p	0.8297		0.0166	

See also Supplementary Table S1, for list of ROIs in each network. Mod/Poor, moderate/poor response level; ROI, region of interest.

In addition, P6 who had nonfluent aphasia (13 years poststroke) showed significant increase in number of different verbs used to describe the BDAE Cookie Theft Picture[43] post-LED Protocol D. His baseline mean for number of different verbs used was 6.3 (SD, 0.58); at 1 month post-LED, number of different verbs was 9; and at 2 months post-LED, number of different verbs was 11—for example, almost double the number of different verbs from baseline. Supplemental language data for P6 are shown in Supplementary Figs. S2–S4.

Figure 6 shows the paired *t*-test results in bar graph form for Pearson's *r* correlations transformed into z-scores, for the three separate intrinsic neural networks (DMN, SN, and CEN), pre/post Protocols C and D. Although *pre-LED* there were no significant differences in functional connectivity within each of the three networks for those treated with Protocol C versus Protocol D, *post-LED* there were significant differences in functional connectivity within each of the three networks for those treated with Protocol C versus Protocol D, where significant *increased* functional connectivity was present following Protocol D.

Discussion

Part 1

The overt picture-naming *task-fMRI* scans with P1 are the first to show different behavioral effects with different tLED placement locations in chronic stroke. In Part 1, Protocol A showed that bilateral (LH and RH) application of the LED cluster heads, including both L and R SMAs (midline, vertex of the head), did not improve naming. Protocol B, however, showed that LED application to *only the LH, ipsilesional side* of the head where the stroke had occurred, was associated with significant increase in post-LED naming ability. The overt picture-naming *task-fMRI* scans also showed different patterns of activation for Protocol A versus Protocol B. After bilateral LED application (Protocol A), the fMRI scans showed bilateral activation—for example, LH, perilesional activation, as well as overall RH activation, including both the L and R SMAs. In aphasia recovery studies with fMRI scans, higher activation in the L SMA than in the R SMA (and not high activation in both SMAs) has been associated with better language recovery.[48,49] High fMRI activation in the RH, in LH stroke patients with

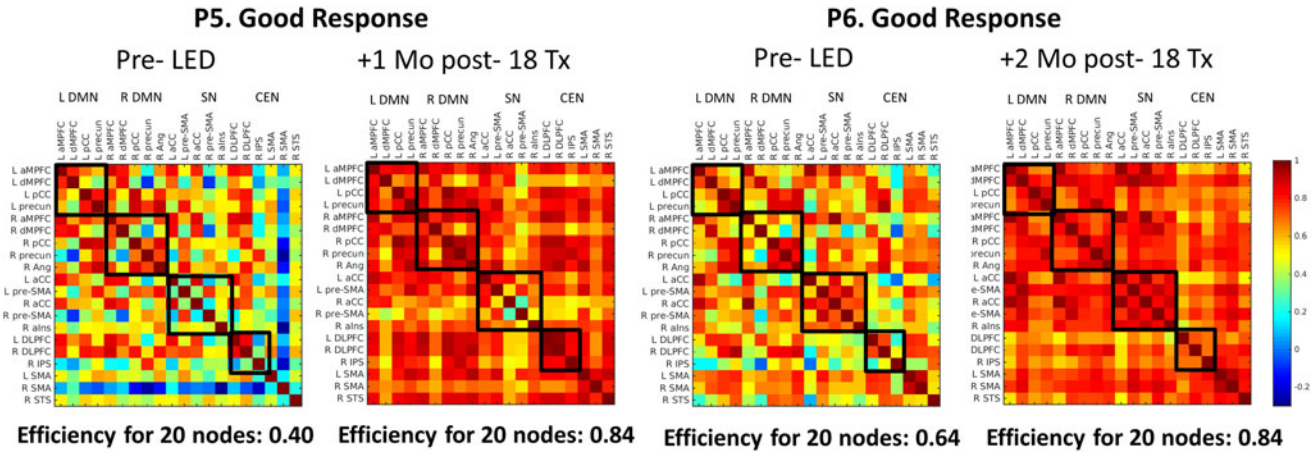

FIG. 5. Part 2: Pre/post rs-fcMRI correlation matrices for 20 cortical ROIs for Protocol D, for P5 and P6, both GR cases (Table 5, bottom, naming test scores). These two cases showed significant increase in functional connectivity within the DMN, SN, and CEN, post-18 tLED treatments (Table 6). With Protocol D, the LED cluster heads were placed only on the LH ipsilesional side, *plus two midline nodes of the DMN*—for example, mPFC and precuneus *simultaneously*, with 26 J/cm^2 per LED placement. The *pre-LED* node efficiency for the 20 ROI nodes ranged from 0.40 (P5) to 0.64 (P6). The *post-LED* efficiency increased for P5 to 0.84 (change of +0.44), and for P6, it also increased to 0.84 (change of +0.20). GR, good response.

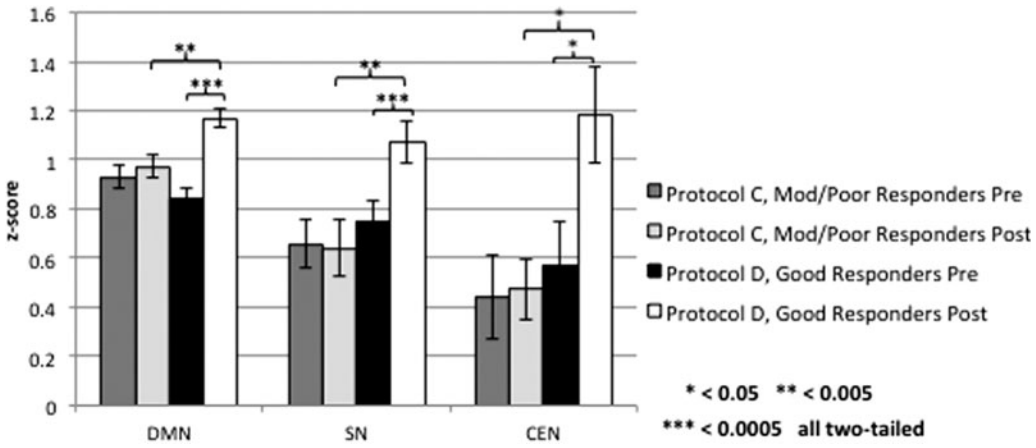

FIG. 6. Part 2: Bar graphs showing paired *t*-test results for Pearson's *r* correlations transformed into z-scores for ROIs in the intrinsic neural networks—for example, default mode, salience and central executive, pre-/post-LED Protocols C and D. Protocol C, wherein there was only MR/PR in naming post-LED (P3, P4), showed no significant changes post-LED in functional connectivity in the DMN, SN, or CEN. Protocol C had treated only the LH, ipsilesional side, *plus one midline node on the DMN* (mPFC) using 13 J/cm^2. Protocol D, however, wherein there was GR in naming post-LED, P5 and P6 showed significant increase post-LED in functional connectivity within the DMN, SN, and CEN. Protocol D had treated only the LH ipsilesional side, *plus two midline nodes on the DMN* (mPFC and precuneus) using 26 J/cm^2. Although there were no significant differences *pre-LED* in functional connectivity within each of the three networks for those treated with Protocol C versus Protocol D, there were significant differences *post-LED* in functional connectivity within each of the three networks for those treated with Protocol C versus Protocol D, with greater functional connectivity in the latter.

nonfluent aphasia, has been considered a maladaptive pattern, likely due to less transcallosal inhibition from the damaged dominant L frontal areas.[50–55] Multiple studies with repetitive transcranial magnetic stimulation (rTMS) have shown that suppression of the R pars triangularis (pTr) in the R inferior frontal gyrus, with 1 Hz rTMS in chronic nonfluent aphasia, has significantly improved naming.[56,57] Overt picture-naming *task-fMRI* scans after a series of rTMS treatments to suppress the R pTr area have shown increased LH activation along with improved naming in nonfluent aphasia.[58]

For Protocol B, the overt picture-naming *task-fMRI* scans showed primarily only LH activation (not RH activation), and only L SMA activation (not R SMA), despite no direct LED treatment of the L SMA. Connections between the L SMA and the L inferior gyrus, pars opercularis, a posterior portion of L Broca's area, have been documented using the diffusion tensor MRI method.[59] Connections between motor cortex and SMA are well established. Activation of the L SMA is important for motor speech initiation. P1 had minimal lesion in the L motor cortex area for mouth. Hence, it is likely that at least some connections between the L motor cortex and the L SMA were preserved, promoting the increased L SMA activation after LED placements to only the LH perisylvian cortical areas (including the L motor cortex area) in Protocol B, with P1.

Several functional imaging studies in aphasia have reported increased LH activation to be associated with better language recovery after language therapy.[60–65] The role of the RH in recovery from aphasia may be beneficial, however, when a large lesion is present in LH language areas.[66,67] However, increased RH activation was not associated with improved naming post-bilateral tLED placements in this tPBM study.

These results suggest that at least some NIR photons from the LEDs were penetrating through scalp, bone, and meninges to reach specific surface brain cortex areas at an adequate amount to promote beneficial change in the remaining (perilesional) parts of the LH neural network for language, when only the LH was treated (Protocol B). The *different* post-LED fMRI cortical activation patterns for Protocol B versus Protocol A were parallel to the changes in naming ability following Protocol B versus Protocol A. These specific effects from tPBM on language (and fMRI scans) are in fact analogous to previously known effects from other noninvasive treatment methods—for example, rTMS and language therapy, wherein improved language and improved activation in the LH on fMRI scans were present. The parallel patterns observed between tPBM and other noninvasive treatment methods suggest that the NIR photons applied on the scalp were reaching the targeted subjacent surface brain cortex areas.

Part 2

These rs-fcMRI scans are the first to show significant increased functional connectivity in neural networks, in chronic stroke patients after a series of tPBM treatments. In Part 2, rs-fcMRI scans were used to examine functional connectivity in domain-general (not language-specific) intrinsic neural networks after a series of tLED treatments to only the LH ipsilesional side *plus* additional LED placement/s over specific midline cortical node/s of the DMN. When LEDs were placed on only the LH ipsilesional side, plus over *one midline node of the DMN* (mPFC), however, there was only MR or PR in naming, and no significant increase in functional connectivity within the DMN, SN, or CEN. When LEDs were placed on only the LH ipsilesional side, plus over *two midline nodes of the DMN* (mPFC and precuneus, *simultaneously*), there was GR, with significant increase in naming for both PWA, and there was significant

increase in functional connectivity within the intrinsic neural networks—DMN, SN, and CEN.

Positive results after the additional midline LED placement over the precuneus cortical node of the DMN are parallel to previous aphasia research wherein the role of the precuneus was observed to be especially important within the DMN in aphasia patients who responded well to a series of language treatments for anomia.[68] The role of the precuneus during cognitive tasks with normal subjects is also well known.[69] Abnormalities in the DMN have been reported in acute stroke patients,[70] as well as in subacute stroke patients.[71] Improvements in the DMN have been reported in stroke patients with better recovery in cognition at 2 or 3 months poststroke.[72]

Marcotte et al.[73] were the first to study the DMN with rs-fcMRI scans in *chronic* aphasia patients, ranging from 4 to 25 years poststroke. They examined pre/post changes in the DMN after a language therapy program for anomia, based on semantic feature analysis. They observed improved integration of the posterior parts of the DMN, but this change was not significantly correlated with changes post-therapy in naming, for their nine aphasia patients. They did suggest, however, that at least some *pre-therapy* integration of the DMN may predict therapy outcomes, and strongly recommended additional studies of the DMN in aphasia. Citing Kelly et al.,[74] a higher DMN functional connectivity at rest would favor network efficiency. Network efficiency refers to the connectedness of the edges for the ROIs examined.

In this study, the network efficiency data for the 20 ROIs in the rs-fcMRI correlation matrices (Figs. 4 and 5) suggest that examining pre-LED efficiency might inform ''potential'' for improvement after tLED treatments. For example, the efficiency data pre-LED for P3 and P4 were only 0.39 and 0.31, respectively, and these two cases had only MR/PR following Protocol C. However, the efficiency data pre-LED for P5 and P6 were 0.40 and 0.64, respectively, and these two cases each had GR after LED placements on the LH, plus two nodes of the DMN (Protocol D).

The PWA who had no change in naming post-LED, PR case P4, had the lowest efficiency pre-LED (0.31), and the PWA who had the most improvement in naming post-LED, GR case P6, had the highest efficiency pre-LED (0.64). P4 had a history of severe depression and required 12 weeks to complete the 18 tLED treatments, compared with 6–7 weeks for the other participants. The pre-LED network efficiency for MR case P3 (0.39) and for GR case P5 (0.40) was very close. More studies would be necessary to learn whether rs-fcMRI efficiency data pre-LED might serve as a biomarker for potential improvement post-LED.

The importance of domain-general intrinsic neural networks, including the DMN, SN, and CEN to aphasia recovery has been emphasized.[75,76] Those authors concluded that impaired attention and executive function (associated with poor functional connectivity in these three intrinsic networks) interfered with language recovery—for example, *oral picture description*. In this study, GR case P5 showed significant improvement on both of the two verbal fluency/category-naming tests (requiring executive function) post-Protocol D. The GR case P6 showed significant improvement on the two picture-naming tests, as well as on *oral picture description* wherein he nearly doubled the number of different verbs, and total verbs spoken (BDAE Cookie Theft Picture),[43] post-Protocol D. Language improvements for GR cases P5 and P6 were parallel to significant increases in functional connectivity within the three intrinsic networks (DMN, SN, and CEN). Increases in functional connectivity within these three intrinsic networks may also have contributed to better language recovery by possibly improving executive function and attention.

A stronger deactivation of the DMN is present during a speech production task than during listening to speech in normal subjects.[77] Hence, there is motivation to further study the effect of tPBM applied over midline cortical nodes of the DMN, as well as the LH, strengthening both the DMN and the remaining LH language network to improve speech output in aphasia.

A recent pilot trial that included rs-fcMRI scans in dementia cases wherein NIR tLEDs were placed *only over the cortical nodes of the DMN* showed significant improvement in cognition, as well as increased functional connectivity within the DMN between the posterior cingulate cortex and lateral parietal nodes, after 12 weeks of tLED.[25] Thus, the rs-fcMRI results from this study with chronic stroke patients, and those from the Chao study with chronic dementia cases,[25] suggest that tPBM can increase functional connectivity within neural networks. The NEST clinical trial studies with tPBM to treat *acute* stroke patients were initially successful.[33–35] However, the Phase III trial was suspended at the half-way point due to lack of significance. Possible factors contributing to this may be that (1) both sides of the head were treated regardless of the side of stroke, (2) midline nodes of the DMN were not treated, and (3) only one tPBM treatment was administered. The rs-fcMRI results from this study with *chronic* stroke, and those of Chao with chronic dementia,[25] suggest that a clinical trial with *acute* stroke patients would still be indicated, but using a tPBM protocol different from that of the NEST studies—for example, treatment of only the ipsilesional side of the stroke (not bilateral), plus two midline nodes of the DMN, and at least 18 tPBM treatments.

Two of the PWA (P1, P5) in this study had unique characteristics deserving comment. P1, who had nonfluent aphasia (treated in this LED study at 18 years poststroke), had made significant improvements in naming when treated 10 years earlier (at 8 years poststroke) with rTMS to suppress the R pTr.[58] He still made significant improvements in naming, however, after tLED treatments to only the LH (Protocol B) in this study. Future studies may sequentially use tPBM *plus* rTMS for maximum improvements. Concurrent language therapy along with rTMS has also further improved language.[56] Thus, combining language therapy *plus* tPBM might also maximize language recovery.

P5 had a rare type of aphasia, *unilateral* word deafness, yet he still improved in verbal fluency/category naming when treated with Protocol D, at 11 years poststroke. Word deafness is a type of aphasia that is usually associated with bilateral temporal lobe lesions, involving the superior temporal gyrus of the LH (Wernicke's area, auditory association cortex) and the RH superior temporal gyrus.[78] These PWA hear speech and environmental sounds, but cannot comprehend or identify them; they rely more on writing and reading to communicate—often using closed caption for videos. A shower of emboli can cause this unusual combination of bilateral temporal lobe lesions. P5 had suffered only a single

L temporoparietal stroke (tissue plasminogen activator, tPA was used). The cortical area of infarction included L Wernicke's area (posterior two-thirds, L superior temporal gyrus) with deep extension to include white matter at the posterior rim of the body of the L lateral ventricle, interrupting auditory pathways from the right superior temporal gyrus to the left, crossing the corpus callosum.[79] The structural MRI for P5 is shown in Fig. 1, and in more detail in Supplementary Fig. S1. The final behavioral effect of this unilateral LH lesion was the same as if there had been two separate lesions—for example, one in the LH and one in the RH, superior temporal gyrus areas. Despite this bilateral lesion effect with only a single LH lesion, this patient showed significant improvement in verbal fluency/category naming, when tLED treatments were applied only to the ipsilesional LH side plus two midline nodes of the DMN, 26 J/cm^2 (Protocol D).

LED parameters

PW or continuous wave (CW) was used in the four LED protocols. In Part 1, pulsed LEDs (146 Hz) were used, and in Part 2, only CW was used. Results did not show an advantage of using PW over CW (Supplementary Data S2). The PW rates were used with complete safety, even though a few of the stroke patients already had a history of seizures, and were on antiseizure medications before they entered this study. No seizures occurred.

The total fluence (sum of total Joules/cm^2) applied across the 18 tLED sessions for each of the four LED treatment protocols is listed in Tables 2 and 3. These values suggest that when a higher fluence was applied, better results were observed—that is, the two LED protocols without significant improvements (A and C) had total applications of <3000 J/cm^2 (Protocol A, 2800 J/cm^2; Protocol C, 2100 J/cm^2). The two LED protocols with significant improvements (B and D), however, each had a total application of >3700 J/cm^2 (Protocol B, 4212 J/cm^2 and Protocol D, 3744 J/cm^2). In this study with PWA who had LH stroke, however, the LED placement locations (LH only) and two placements on the midline, DMN, were also found to be important. More studies with at least a total fluence of 3700 J/cm^2 and appropriate LED placements are indicated with stroke patients.

Limitations of the study

Limitations include small sample size ($n=6$) and heterogeneity among the LH lesion sites and types of aphasia. There were three cases with mild–moderate nonfluent Broca's aphasia (P1, P2, and P6): two cases with recovered nonfluent Broca's aphasia who presented with anomia (P3 and P4) and one fluent case with a rare unilateral word deafness (P5). Overall, there was significant improvement with the three mild–moderate nonfluent Broca's aphasia cases, when the LH was treated with higher levels of fluence per LED cluster head—for example, P1 and P2, with 39 J/cm^2 (Protocol B), and P6, with 26 J/cm^2 (Protocol D). There was also significant improvement for the fluent word deafness PWA, P5, treated with a fluence of 26 J/cm^2 (Protocol D). Thus, significant improvements in naming were observed for nonfluent, as well as for fluent, aphasia when only the LH was treated, and a higher fluence was used, at least 26 J/cm^2 per LED cluster head, and total fluence was at least 3700 J/cm^2.

The possible effect of the suboccipital LED placement also deserves mention. There was one midline LED placement, inferior to the occipital protuberance over the midline cerebellum area used in Protocol D. The effect is unknown. This placement was part of the original LED treatment protocol used with TBI, and it was initially chosen to possibly increase rCBF to the cerebellum, and possibly promote vasodilation for the vertebral and basilar arteries. Placement of an LED on the midline cerebellum was also part of Protocols A and C, however, and neither of these two protocols was associated with significant improvements in naming. Protocol A had used bilateral placements (total fluence was only 2808 J/cm^2). Protocol C had used only 13 J/cm^2 on each LED cluster head, over the LH plus only *one* node of the DMN, mPFC (total fluence was only 2106 J/cm^2). Thus, although the midline cerebellum placement may have contributed to overall better naming following Protocol D, the relative effect of the suboccipital placement is unknown, but deserves further study.

Conclusions

This tPBM study supports the ideas of Dijkhuizen et al.[80] regarding recovery and rehabilitation in stroke: ''Restoration of functional connectivity in surviving networks is critical for functional recovery, and may be promoted with specific therapeutic strategies such as …noninvasive brain stimulation'' (p. 638). Application of NIR tPBM may serve as a new form of noninvasive brain stimulation that can promote better neuromodulation poststroke, thus adding another therapeutic modality for poststroke treatment.

Additional fMRI studies to examine the effects of transcranial NIR photons applied to specific cortical brain areas in stroke and in other CNS disorders are warranted. Different tPBM treatment protocols are likely indicated for different CNS disorders—for example, ipsilesional for stroke, but bilateral for TBI/PTSD and AD/dementia. Also, the possibility for tLED to increase functional connectivity through targeted application over at least *two*, cortical nodes within an intrinsic neural network *simultaneously* (perhaps simultaneously strengthening a targeted neural connection) during, and after a series of tPBM treatments, may be a unique feature of tPBM that deserves further exploration.

Acknowledgments

The authors thank Andrea Fedoruk for invaluable assistance with article preparation; Ethan Treglia, MS, CCC-SLP, for language testing; and Ronald J. Killiany, PhD, Director, Boston University Center for Biomedical Imaging, and Andy Ellison, MR Technologist, for assistance with MRI acquisition. The MedX Health LED equipment was purchased through funding from the Boston VA Research Institute (BVARI); the authors thank Anita Saltmarche, BScN, MHSc, for assistance with MedX Health, Toronto. The research was supported by the Department of Veterans Affairs. NCT: NCT00467103.

Authors' List for Potential Conflict of Interest

Dr. Hamblin is on the following scientific advisory boards: Transdermal Cap, Inc., Cleveland, OH; BeWell Global, Inc., Wan Chai, Hong Kong; Hologenix, Inc., Santa

Monica, CA; LumiThera, Inc., Poulsbo, WA; Vielight, Toronto, Canada; Bright Photomedicine, Sao Paulo, Brazil; Quantum Dynamics LLC, Cambridge, MA; Global Photon, Inc., Bee Cave, TX; Medical Coherence, Boston, MA; NeuroThera, Newark, DE; JOOVV, Inc., Minneapolis-St. Paul, MN; AIRx Medical, Pleasanton, CA; FIR Industries, Inc., Ramsey, NJ; UVLRx Therapeutics, Oldsmar, FL; Ultralux UV, Inc., Lansing, MI; Illumiheal & Petthera, Shoreline, WA; MB Lasertherapy, Houston, TX; and ARRC LED, San Clemente, CA.

Dr. Hamblin has been a consultant for Lexington Int, Boca Raton, FL; USHIO Corp., Japan; Merck KGaA, Darmstadt, Germany; Philips Electronics, Nederland B.V.; Johnson & Johnson, Inc., Philadelphia, PA; and Sanofi-Aventis Deutschland GmbH, Frankfurt am Main, Germany.

Dr. Hamblin is a stockholder in Global Photon, Inc., Bee Cave, TX, and Mitonix, Newark, DE.

Dr. Naeser's research has received funds from Vielight, Inc., Toronto, Ontario, Canada.

Author Disclosure Statement

No competing financial interests exist.

Author Contributions Statement

M.A.N., M.D.H., and P.I.M. initiated and designed the overall study, including the pre-/post-LED naming tests and the four LED protocols. M.D.H., P.I.M., and B.B.K. designed and analyzed the fMRI portions of the study. M.R.H. consulted on the mechanisms of t-PBM. All authors contributed to writing and reviewing the article.

Funding Information

The MedX Health LED equipment was purchased through funding from the Boston VA Research Institute (BVARI); the authors thank Anita Saltmarche, BScN, MHSc, for assistance with MedX Health, Toronto. The research was supported by the Department of Veterans Affairs. NCT: NCT00467103.

Supplementary Material

Supplementary Data S1
Supplementary Data S2
Supplementary Table S1
Supplementary Figure S1
Supplementary Figure S2
Supplementary Figure S3
Supplementary Figure S4

References

1. Ferraresi C, Kaippert B, Avci P, et al. Low-level laser (light) therapy increases mitochondrial membrane potential and ATP synthesis in C2C12 myotubes with a peak response at 3–6 h. Photochem Photobiol 2015;91:411–416.
2. Karu TI, Pyatibrat LV, Afanasyeva NI. Cellular effects of low power laser therapy can be mediated by nitric oxide. Lasers Surg Med 2005;36:307–314.
3. Wong-Riley MT, Liang HL, Eells JT, et al. Photobiomodulation directly benefits primary neurons functionally inactivated by toxins: role of cytochrome c oxidase. J Biol Chem 2005;280:4761–4771.
4. Schiffer F, Johnston AL, Ravichandran C, et al. Psychological benefits 2 and 4 weeks after a single treatment with near infrared light to the forehead: a pilot study of 10 patients with major depression and anxiety. Behav Brain Funct 2009;5:46.
5. Nawashiro H, Wada K, Nakai K, Sato S. Focal increase in cerebral blood flow after treatment with near-infrared light to the forehead in a patient in a persistent vegetative state. Photomed Laser Surg 2012;30:231–233.
6. Hipskind SG, Grover FL, Fort R, et al. Pulsed transcranial red/near-infrared light therapy using light-emitting diodes improves cerebral blood flow and cognitive function in veterans with chronic traumatic brain injury: a case series. Photomed Laser Surg 2018 [Epub ahead of print]; DOI: 10.1089/pho.2018.4489.
7. Naeser M, Ho M, Martin P, et al. Improved language after scalp application of red/near-infrared light-emitting diodes: pilot study supporting a new, noninvasive treatment for chronic aphasia. Procedia Soc Behav Sci 2012;61:138–139.
8. Ho M, Martin P, Yee M, Koo B, Baker E, Hamblin M. Increased functional connectivity in default mode network associated with application of transcranial, light-emitting diodes to treat chronic aphasia: case series. J Int Neuropsychol Soc 2016;22:229.
9. de Freitas LF, Hamblin MR. Proposed mechanisms of photobiomodulation or low-level light therapy. IEEE J Sel Top Quantum Electron 2016;22:348–364.
10. Huang YY, Nagata K, Tedford CE, McCarthy T, Hamblin MR. Low-level laser therapy (LLLT) reduces oxidative stress in primary cortical neurons in vitro. J Biophotonics 2013;6:829–838.
11. Sompol P, Xu Y, Ittarat W, Daosukho C, Clair DS. NF-kappaB-Associated MnSOD induction protects against beta-amyloid-induced neuronal apoptosis. J Mol Neurosci 2006;29:279–288.
12. Zhang YH, Takahashi K, Jiang GZ, et al. In vivo production of heat shock protein in mouse peritoneal macrophages by administration of lipopolysaccharide. Infect Immun 1994;62:4140–4144.
13. De Taboada L, Yu J, El-Amouri S, et al. Transcranial laser therapy attenuates amyloid-beta peptide neuropathology in amyloid-beta protein precursor transgenic mice. J Alzheimers Dis 2011;23:521–535.
14. Hamblin MR. Mechanisms and applications of the anti-inflammatory effects of photobiomodulation. AIMS Biophys 2017;4:337–361.
15. Khuman J, Zhang J, Park J, Carroll JD, Donahue C, Whalen MJ. Low-level laser light therapy improves cognitive deficits and inhibits microglial activation after controlled cortical impact in mice. J Neurotrauma 2012;29:408–417.
16. Thunshelle C, Hamblin MR. Transcranial low-level laser (light) therapy for brain injury. Photomed Laser Surg 2016; 34:587–598.
17. Xuan W, Vatansever F, Huang L, Hamblin MR. Transcranial low-level laser therapy enhances learning, memory, and neuroprogenitor cells after traumatic brain injury in mice. J Biomed Opt 2014;19:108003.
18. Xuan W, Agrawal T, Huang L, Gupta GK, Hamblin MR. Low-level laser therapy for traumatic brain injury in mice increases brain derived neurotrophic factor (BDNF) and synaptogenesis. J Biophotonics 2015;8:502–511.
19. Naeser MA, Zafonte R, Krengel MH, et al. Significant improvements in cognitive performance post-transcranial, red/

near-infrared light-emitting diode treatments in chronic, mild traumatic brain injury: open-protocol study. J Neurotrauma 2014;31:1008–1017.
20. Naeser MA, Martin PI, Ho MD, et al. Transcranial, red/near-infrared light-emitting diode therapy to improve cognition in chronic traumatic brain injury. Photomed Laser Surg 2016;34:610–626.
21. Bonnelle V, Leech R, Kinnunen KM, et al. Default mode network connectivity predicts sustained attention deficits after traumatic brain injury. J Neurosci 2011;31:13442–13451.
22. Zhao J, Tian Y, Nie J, Xu J, Liu D. Red light and the sleep quality and endurance performance of Chinese female basketball players. J Athl Train 2012;47:673–678.
23. Shin LM, Rauch SL, Pitman RK. Structural and Functional Anatomy of PTSD: Findings from Neuroimaging Research. New York, NY: Guilford Press, 2005.
24. Saltmarche AE, Naeser MA, Ho KF, Hamblin MR, Lim L. Significant improvement in cognition in mild to moderately severe dementia cases treated with transcranial plus intranasal photobiomodulation: case series report. Photomed Laser Surg 2017;35:432–441.
25. Chao LL. Effects of home photobiomodulation treatments on cognitive and behavioral function, cerebral perfusion, and resting-state functional connectivity in patients with dementia: a pilot trial. Photobiomodul Photomed Laser Surg 2019;37:133–141.
26. Buckner RL, Sepulcre J, Talukdar T, et al. Cortical hubs revealed by intrinsic functional connectivity: mapping, assessment of stability, and relation to Alzheimer's disease. J Neurosci 2009;29:1860–1873.
27. Greicius MD, Srivasta G, Reiss AL, et al. Default-mode network activity distinguishes Alzheimer's disease from healthy aging: evidence from functional MRI. Proc Natl Acad Sci U S A 2004;101:4637–4642.
28. Petrella JR, Sheldon FC, Prince SE, Calhoun VD, Doraiswamy PM. Default mode network connectivity in stable vs progressive mild cognitive impairment. Neurology 2011;76:511–517.
29. Simic G, Babic M, Borovecki F, Hof PR. Early failure of the default-mode network and the pathogenesis of Alzheimer's disease. CNS Neurosci Ther 2014;20:692–698.
30. Crossley NA, Mechelli A, Scott J, et al. The hubs of the human connectome are generally implicated in the anatomy of brain disorders. Brain 2014;137(Pt 8):2382–2395.
31. Raichle ME. The brain's default mode network. Annu Rev Neurosci 2015;38:433–447.
32. Kosel KC, Van Hoesen GW, West JR. Olfactory bulb projections to the parahippocampal area of the rat. J Comp Neurol 1981;198:467–482.
33. Lampl Y, Zivin JA, Fisher M, et al. Infrared laser therapy for ischemic stroke: a new treatment strategy: results of the NeuroThera Effectiveness and Safety Trial-1 (NEST-1). Stroke 2007;38:1843–1849.
34. Zivin JA, Albers GW, Bornstein N, et al. Effectiveness and safety of transcranial laser therapy for acute ischemic stroke. Stroke 2009;40:1359–1364.
35. Stemer AB, Huisa BN, Zivin JA. The evolution of transcranial laser therapy for acute ischemic stroke, including a pooled analysis of NEST-1 and NEST-2. Curr Cardiol Rep 2010;12:29–33.
36. Eriksson PS, Perfilieva E, Bjork-Eriksson T, et al. Neurogenesis in the adult human hippocampus. Nat Med 1998;4:1313–1317.
37. Jin K, Wang X, Xie L, et al. Evidence for stroke-induced neurogenesis in the human brain. Proc Natl Acad Sci U S A 2006;103:13198–13202.
38. Voloboueva LA, Giffard RG. Inflammation, mitochondria, and the inhibition of adult neurogenesis. J Neurosci Res 2011;89:1989–1996.
39. Wan S, Parrish JA, Anderson RR, Madden M. Transmittance of nonionizing radiation in human tissues. Photochem Photobiol 1981;34:679–681.
40. Tedford CE, DeLapp S, Jacques S, Anders J. Quantitative analysis of transcranial and intraparenchymal light penetration in human cadaver brain tissue. Lasers Surg Med 2015;47:312–322.
41. Uozumi Y, Nawashiro H, Sato S, Kawauchi S, Shima K, Kikuchi M. Targeted increase in cerebral blood flow by transcranial near-infrared laser irradiation. Lasers Surg Med 2010;42:566–576.
42. Mester E, Spiry T, Szende B, Tota JG. Effect of laser rays on wound healing. Am J Surg 1971;122:532–535.
43. Goodglass H, Kaplan E, Barresi B. The Assessment of Aphasia and Related Disorders, 3rd ed. Philadelphia, PA: Lippincott, Williams and Wilkins, 2001.
44. Kaplan E, Goodglass H, Weintraub S. The Boston Naming Test, 2nd ed. Philadelphia, PA: Lea & Febiger, 1983.
45. Roach A, Schwartz, MF, Martin, N, Grewal RS, Brecher A. The Philadelphia Naming Test: scoring and rationale. Clin Aphasiol 1996;24:121–133.
46. Ruff RM, Light RH, Parker SB, Levin HS. Benton Controlled Oral Word Association Test: reliability and updated norms. Arch Clin Neuropsychol 1996;11:329–338.
47. Karu TI, Pyatibrat LV, Esenaliev RO. Effect of monochromatic red and near-infrared light on the adhesive properties of the cell membrane: dependence on wavelength. Bull Exp Biol Med 1994;117:679–681.
48. Heiss WD, Thiel A. A proposed regional hierarchy in recovery of post-stroke aphasia. Brain Lang 2006;98:118–123.
49. Saur D, Lange R, Baumgaertner A, et al. Dynamics of language reorganization after stroke. Brain 2006;129(Pt 6):1371–1384.
50. Belin P, Van Eeckhout P, Zilbovicius M, et al. Recovery from nonfluent aphasia after melodic intonation therapy: a PET study. Neurology 1996;47:1504–1511.
51. Lefaucheur JP. Stroke recovery can be enhanced by using repetitive transcranial magnetic stimulation (rTMS). Neurophysiol Clin 2006;36:105–115.
52. Martin PI, Naeser MA, Doron KW, et al. Overt naming in aphasia studied with a functional MRI hemodynamic delay design. Neuroimage 2005;28:194–204.
53. Naeser MA, Martin PI, Baker EH, et al. Overt propositional speech in chronic nonfluent aphasia studied with the dynamic susceptibility contrast fMRI method. Neuroimage 2004;22:29–41.
54. Postman-Caucheteux WA, Birn RM, Pursley RH, et al. Single-trial fMRI shows contralesional activity linked to overt naming errors in chronic aphasic patients. J Cogn Neurosci 2010;22:1299–1318.
55. Rosen HJ, Petersen SE, Linenweber MR, et al. Neural correlates of recovery from aphasia after damage to left inferior frontal cortex. Neurology 2000;55:1883–1894.
56. Naeser MA, Martin PI, Ho M, et al. Transcranial magnetic stimulation and aphasia rehabilitation. Arch Phys Med Rehabil 2012;93(1 Suppl):S26–S34.

57. Ren CL, Zhang GF, Xia N, et al. Effect of low-frequency rTMS on aphasia in stroke patients: a meta-analysis of randomized controlled trials. PLoS One 2014;9:e102557.
58. Martin PI, Naeser MA, Ho M, et al. Overt naming fMRI pre- and post-TMS: two nonfluent aphasia patients, with and without improved naming post-TMS. Brain Lang 2009; 111:20–35.
59. Ford A, McGregor KM, Case K, Crosson B, White KD. Structural connectivity of Broca's area and medial frontal cortex. Neuroimage 2010;52:1230–1237.
60. Cornelissen K, Laine M, Tarkiainen A, Jarvensivu T, Martin N, Salmelin R. Adult brain plasticity elicited by anomia treatment. J Cogn Neurosci 2003;15:444–461.
61. Fridriksson J, Morrow-Odom L, Moser D, Fridriksson A, Baylis G. Neural recruitment associated with anomia treatment in aphasia. Neuroimage 2006;32:1403–1412.
62. Leger A, Demonet JF, Ruff S, et al. Neural substrates of spoken language rehabilitation in an aphasic patient: an fMRI study. Neuroimage 2002;17:174–183.
63. Meinzer M, Flaisch T, Breitenstein C, Wienbruch C, Elbert T, Rockstroh B. Functional re-recruitment of dysfunctional brain areas predicts language recovery in chronic aphasia. Neuroimage 2008;39:2038–2046.
64. Small SL, Flores DK, Noll DC. Different neural circuits subserve reading before and after therapy for acquired dyslexia. Brain Lang 1998;62:298–308.
65. Rochon E, Leonard C, Burianova H, et al. Neural changes after phonological treatment for anomia: an fMRI study. Brain Lang 2010;114:164–179.
66. Fernandez B, Cardebat D, Demonet JF, et al. Functional MRI follow-up study of language processes in healthy subjects and during recovery in a case of aphasia. Stroke 2004;35:2171–2176.
67. Skipper-Kallal LM, Lacey EH, Xing S, Turkeltaub PE. Right hemisphere remapping of naming functions depends on lesion size and location in poststroke aphasia. Neural Plast 2017;2017:8740353.
68. Fridriksson J, Moser D, Bonilha L, et al. Neural correlates of phonological and semantic-based anomia treatment in aphasia. Neuropsychologia 2007;45:1812–1822.
69. Utevsky AV, Smith DV, Huettel SA. Precuneus is a functional core of the default-mode network. J Neurosci 2014; 34:932–940.
70. Carter AR, Astafiev SV, Lang CE, et al. Resting interhemispheric functional magnetic resonance imaging connectivity predicts performance after stroke. Ann Neurol 2010;67:365–375.
71. Tuladhar AM, Snaphaan L, Shumskaya E, et al. Default mode network connectivity in stroke patients. PLoS One 2013;8:e66556.
72. Park JY, Kim YH, Chang WH, et al. Significance of longitudinal changes in the default-mode network for cognitive recovery after stroke. Eur J Neurosci 2014;40:2715–2722.
73. Marcotte K, Perlbarg V, Marrelec G, Benali H, Ansaldo AI. Default-mode network functional connectivity in aphasia: therapy-induced neuroplasticity. Brain Lang 2013;124: 45–55.
74. Kelly AM, Uddin LQ, Biswal BB, Castellanos FX, Milham MP. Competition between functional brain networks mediates behavioral variability. Neuroimage 2008;39:527–537.
75. Brownsett SL, Warren JE, Geranmayeh F, Woodhead Z, Leech R, Wise RJ. Cognitive control and its impact on recovery from aphasic stroke. Brain 2014;137(Pt 1):242–254.
76. Geranmayeh F, Brownsett SL, Wise RJ. Task-induced brain activity in aphasic stroke patients: what is driving recovery? Brain 2014;137(Pt 10):2632–2648.
77. van de Ven V, Esposito F, Christoffels IK. Neural network of speech monitoring overlaps with overt speech production and comprehension networks: a sequential spatial and temporal ICA study. Neuroimage 2009;47:1982–1991.
78. Buchman AS, Garron DC, Trost-Cardamone JE, Wichter MD, Schwartz M. Word deafness: one hundred years later. J Neurol Neurosurg Psychiatry 1986;49:489–499.
79. Damasio H, Damasio A. ''Paradoxic'' ear extinction in dichotic listening: possible anatomic significance. Neurology 1979;29:644–653.
80. Dijkhuizen RM, Zaharchuk FR, Otte WM. Assessment and modulation of resting-state neural networks after stroke. Curr Opin Neurol 2014;27:637–643.
81. Naeser MA, Palumbo CL, Helm-Estabrooks N, Stiassny-Eder D, Albert ML. Severe nonfluency in aphasia. Role of the medial subcallosal fasciculus and other white matter pathways in recovery of spontaneous speech. Brain 1989; 112(Pt 1):1–38.
82. Catani M, Mesulam MM, Jakobsen E, et al. A novel frontal pathway underlies verbal fluency in primary progressive aphasia. Brain 2013;136(Pt 8):2619–2628.
83. Siedentopf CM, Golaszewski SM, Mottaghy FM, Ruff CC, Felber S, Schlager A. Functional magnetic resonance imaging detects activation of the visual association cortex during laser acupuncture of the foot in humans. Neurosci Lett Jul 12 2002;327:53–56.

Address correspondence to:
Margaret A. Naeser, PhD
VA Boston Healthcare System (12-A)
Jamaica Plain Campus
150 So. Huntington Avenue
Boston, MA 02130

E-mail: mnaeser@bu.edu

Received: January 26, 2019.
Accepted after revision: July 14, 2019.
Published online: September 24, 2019.